Journal of Energy Storage 27 (2020) 101045

Contents lists available at ScienceDirect

Journal of Energy Storage

journal homepage: www.elsevier.com/locate/est

Numerical and experimental analysis on thermal energy storage of polyethylene/functionalized graphene composite phase change materials

Santosh Chavan, Veershetty Gumtapure, Arumuga Perumal D*

Department of Mechanical Engineering, National Institute of Technology Karnataka, Surathkal, Mangalore -575025, India

ARTICLE INFO

Keywords:
Composite phase change materials
Thermal storage material (TSM)
Thermal energy storage (TES)
Linear low-density polyethylene (LLDPE)
Melting and Solidification

ABSTRACT

The main driving force behind the present work is environmental issues caused due to the usage of plastics, and energy issues. Current work attempts to address these problems by converting recycled plastics into thermal storage materials (TSM). Unfavorable thermophysical properties of plastic make it impractical but these inadequacies can be amended by blending with additives of superior thermophysical properties like, functionalized graphene. Numerical and experimental analysis are carried out to assess the thermal performance of TSMs (LLDPE, CPCM-1, CPCM-2 and CPCM-3) and check the compatibility of the materials. The phase change temperature of TSM is 123 to 125 °C and heat of fusion is 71.95 to 97 kJ/kg. Several thermal characteristics are analyzed to assess thermal performance and the amount of heat energy supplied, rate of heat transfer, and heat storage efficiency are deliberated. Results shown energy level enhancement of 43.17, 50.42, 54 and 50.61% for LLDPE, CPCM-1, CPCM-2 and CPCM-3 respectively. Among the TSM CPCM-2 shows relatively better storage capability (54% enhancement) due to incorporation of optimum concentration of enhancing material. The solidification process takes place through convection and radiation mode of heat transfer, at the completion of solidification process the TSM energy content reduces to 97.5, 96, 96 and 96% for LLDPE, CPCM-1,CPCM-2 and CPCM-3 respectively. This work concludes that, recycled plastics can be blended and it can be converted into efficient thermal storage material.

1. Introduction

Energy conservation and pollution control is a major concern in worldwide due to increase in global warming over the past few decades. The scientific community is also apprehensive about environmental issues caused by the usage of plastics and energy issues. Phase change material (PCM) based thermal energy storage technologies are encouraged as an alternative energy utilization opportunity [1]. The mismatch between the solar thermal energy availability and the demand thrusts towards the new possibilities. Among several energy conservation methods, thermal energy storage (TES) is one of the proficient ways that bridge the intermittency of solar thermal energy. TES can be achieved by different methods such as sensible, latent and thermochemical heat storage. Among the methods, latent heat storage provides better results due to its isothermal in nature. Sensible heat storage causes change in temperature whereas latent heat is stored during phase conversion. Latent heat storage is an effective way due to its high energy storage density at constant temperature. In latent heat storage method selection of suitable material plays a significant role to address the thermal energy utilization [2].

Plastics are becoming a vital asset of humanity due to its wide range of applications and feasibility that cannot be easily or economically replaced by other materials [3]. Plastic usage is almost unavoidable in the present-day scenario even though it is a major toxic pollutant. To overcome the problem of intrinsic toxicity of polyethylene (plastic), it is possible to modify these materials and use as a TES media. Recycled high-density polyethylene (HDPE) is a low-cost material with melting temperature of 125 °C, and latent heat of 210–220 J/g, which can be used for TES material. To provide more feasibility to the material usage, HDPE is also used with material combinations such as poly lactic acid (PLA), paraffin wax, polyethylene glycol etc. The blending of suitable materials with HDPE phase avoids the risk of leakage problem during phase conversion [4]. Recent studies on different combinations of materials focuses the development of thermal storage materials to enhance the overall performance of the TES system. However, their thermophysical properties vary with mass concentrations, thermal conductivity, phase change behavior, heat capacity, and the equivalent thermodynamic response are not investigated extensively [5]. Low thermal conductivity, poor thermal stability, high flammability, supercooling, corrosiveness, and leakage during phase change processes

* Corresponding author.
E-mail address: perumal@nitk.edu.in (A.P. D).

https://doi.org/10.1016/j.est.2019.101045
Received 10 August 2019; Received in revised form 13 October 2019; Accepted 27 October 2019

are confines the feasibility of PCMs [6,7]. The CPCMs based on LDPE, LLDPE and HDPE blended with soft paraffin wax are investigated, and wax contents influences the melting and solidification characteristics. The waxes are uniformly dispersed in the polymer matrix without any leakage [8,9]. Scientific society is continuously focusing on improving the thermophysical properties of PCMs for making it feasible and commercial. Nanocomposite preparation by incorporation of high aspect ratio nanoparticles has provided enhanced thermophysical properties. Carbon-based nanoparticles such as expanded graphite (EG), carbon nanotubes (CNT), fullerene, graphene, graphene fibers etc. shown most favorable results for enhancing the thermophysical properties [10]. Linear low-density polyethylene and ethylene–propylene–-diene terpolymer (EPDM) blend also shown enhanced thermophysical properties and, LLDPE ethylene vinyl acetate (LLDPE/EVA) blends shown reduction in activation energy [11,12]. Thermal storability of the composite improves the combination with LLDPE, paraffin wax, and expanded graphite [13]. The CPCMs have the potential of energy conservation in buildings at different environmental conditions such as a wall coating of CPCM significantly reduces the power consumption by reducing the temperature inside [14,15]. Thermal efficiency can be improved by incorporating nanoparticles into the working fluid to maintain the indoor temperature [16,17]. The domestic applications of CPCMs also extensively used for different industrial applications by heat storage, cooling systems, and textiles due to its isothermal in nature [18,19]. The steady-state and transient heating conditions, are attained with an increase in operating cycles with constant temperature [20,21]. The thermal performance improvement ratios, operation time, heat storing duration, thermal capacity can be achieved by the incorporation of enhancing materials [22,23]. The present-day challenge is to tackle the energy issues and pollution due to plastic usage by utilizing the recycled plastics for TES applications. In the present work, an attempt is made to address the two major worldwide concerned issues by using waste plastics as the thermal energy storage material.

2. Numerical modeling

The thermal energy storage (TES) model considered is a square prism domain of 15 cm × 5 cm × 15 cm (x, y, z) dimensions. Composite phase change material (CPCM) is used as thermal storage material (TSM) in the numerical study. Constant heat flux is applied to the base wall of the domain and all the walls are insulated. Geometrical representation of the computational domain as shown in Fig. 1.

2.1. Numerical model description

To obtain the realistic results assumptions are made for study such as, (a) the molten TSM acts as Newtonian fluid and the flow is incompressible, (b) The phase conversion takes place in laminar form with least viscous dissipation rate, (c) The thermophysical properties of TSM are temperature dependent, (d) Conduction and convection heat transfer rates are controlled, (e) Volume remains same during phase conversion, and (f) the TSM always remains in contact with the boundary walls of the domain [24].

2.2. Boundary conditions

The numerical study is carried out for four different by imposing the constant heat flux boundary condition at the base wall, and remaining walls are insulated. All the four materials are investigated and observed the thermophysical property variation and thermal energy storage capacity during melting and solidification process.

2.3. Mesh independent study

A detailed grid independent study is carried out to find optimum element size for the computational investigation. The maximum temperature obtained after 1500 s is considered for grid independence results comparison. Table 1 shows a comparison of maximum temperature after 1500 s of computational time. The least percentage deviation value is chosen to be the optimum element size and selected for further numerical calculations.

2.4. Numerical methodology

The governing equations used are:
Continuity equation:

$$\frac{\partial u}{\partial x} + \frac{\partial v}{\partial y} = 0 \tag{1}$$

x - Momentum equation:

$$\frac{\partial u}{\partial t} + u\frac{\partial u}{\partial x} + v\frac{\partial u}{\partial y} = -\frac{1}{\rho}\frac{\partial p}{\partial x} + \frac{\mu}{\rho}\left(\frac{\partial^2 u}{\partial x^2} + \frac{\partial^2 u}{\partial y^2}\right) \tag{2}$$

y - Momentum equation:

$$\frac{\partial v}{\partial t} + u\frac{\partial v}{\partial x} + v\frac{\partial v}{\partial y} = -\frac{1}{\rho}\frac{\partial p}{\partial y} + \frac{\mu}{\rho}\left(\frac{\partial^2 v}{\partial x^2} + \frac{\partial^2 v}{\partial y^2}\right) + g\,\beta(T - T_{ref}) \tag{3}$$

Energy equation:

$$\frac{\partial T}{\partial t} + u\frac{\partial T}{\partial x} + v\frac{\partial T}{\partial y} = \alpha\left(\frac{\partial^2 T}{\partial x^2} + \frac{\partial^2 T}{\partial y^2}\right) \tag{4}$$

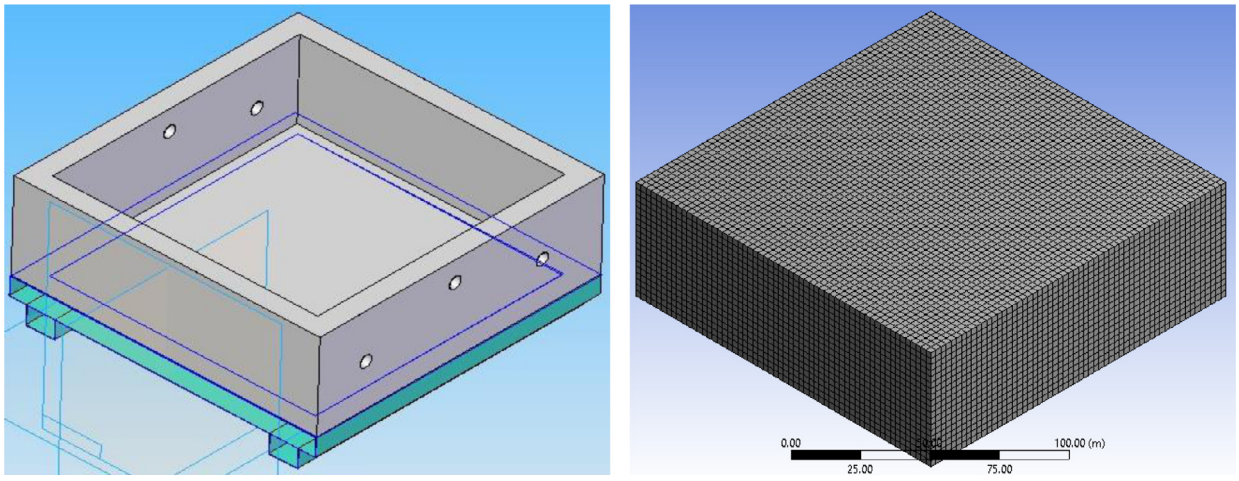

Fig. 1. Geometrical representation of the computational domain.

Table 1
Comparison of maximum temperature after 1500s for different element sizes of the domain.

Element size (mm)	Number of cells	Maximum temperature after 1500 s	% Deviation
4.0	17,797	1205.000	47.50
3.5	36,864	644.241	1.83
3.0	38,416	682.241	7.30
2.5	69,620	644.240	1.83
2.0	140,625	632.390	Base

Where ρ is density, μ is viscosity of the CPCM, p is pressure, g is gravity, β is coefficient of volumetric expansion, T and T_{ref} are medium temperature and reference temperature respectively.

2.5. Computational methodology

The geometrical model is developed by using ANSYS WORKBENCH 16.0 a pre-processing module, to achieve greater accuracy good quality mesh is generated all over the computational domain. To further solve the governing equations, the meshed model is imported to FLUENT 16.0, and related parameters are defined. Composite material properties are added to the FLUENT 16.0 database, and boundary conditions are imposed. FIRST ORDER UPWIND differential scheme is adopted to solve the momentum and energy equations, and PRESTO scheme is used for solving the pressure correction equation. The under-relaxation factors are 0.3, 0.5 and 1.0 for pressure correction, velocity components and thermal energy respectively. The convergence criteria set to 10^{-6} for continuity and momentum equations and 10^{-9} for thermal energy. To obtain the superlative results an optimum element size is chosen through grid independent study.

2.6. Numerical model validation

To validate the present results, existing results of Khodadadi et al. in a square geometry is compared for two different time durations. The boundary conditions imposed are left and right walls are isothermal at 330 K and 300 K, and top and bottom walls are insulated. Fig. 2 shows the streamline patterns of present and existing results [25]. It is observed that as time increases the melting fraction also increases. The streamlines patterns of 500 and 1000 s are found to be similar, and matching with existing results.

3. Thermal energy storage analysis through experimental study

The experimental setup consists a thermal storage unit (TSU) completely filled with composite phase change material. The melting temperature of the CPCMs used in this experiment is in range of 120–125 °C. The CPCM is contained in a stainless-steel unit which can withstand much higher temperature and also a cost-effective material.

3.1. Experimental setup used for thermal energy storage evaluation

Fig. 3(a) and (b) shows the schematic of the complete block diagram of experimental setup and actual representation of components. The TSU is coupled with measuring and controlling devices which are voltage regulator, electric heater, data acquisition system and finally a computer unit to process the obtained data.

3.2. Experimental procedure for thermal performance evaluation

Initially CPCM is filled in the thermal storage unit in the experiment same as numerical analysis. All thermocouples are inserted at appropriate positions, and top face is closed with transparent glass to visualize the melting and solidification processes. A 250 W heat supply is set by adjusting the current and voltage in the voltage regulator unit. The complete set up is perfectly insulated by packing with glass wool, and all thermocouples are connected to the calibrated DAQ. The DAQ is connected to computer unit for data collection and analysis.

3.2.1. Experimental setup components

The present experimental setup contains seven different components as shown in Fig. 4(a)-(d).

(i) **Power supply**
The first component of the TES system is the power supply which is the primary source for running all the equipment. AC supply of 230 V 50 Hz, is used but it can be changed to the required voltage range for running different types of devices.

(ii) **Voltage regulator unit**
Adjustable DC power supply of AC220V 50/60 Hz input, Voltage (0–150) VDC, current (0–2)A, maximum power 300 W (PROXIM ASIA INC) voltage regulator is used to control the supply, as the voltage and current set to provide the required wattage (as shown in Fig. 4(a)).

(iii) **Electric ceramic heater**
A ceramic heating plate (Pragati Ceramics, Gujarat, India) is used to provide uniform surface temperature up to 800 °C, and the maximum heating capacity of the heater is 1 kW. The heating rate is varied by voltage regulator, large grooves are allowed to heat the plate uniformly with low watt density, and high wattage per square inch of radiating surface. The heating elements are fixed in ceramic in different shapes and size depends on the requirements. The heater plate is widely used from low to high voltage due to its cost-effective, energy efficient and environment-friendly in nature (as shown in Fig. 4(b)).

(iv) **Data acquisition system (DAQ)**
The NI 9213 is used to record and analyze the experimental data, the NI 9213 reads and it transfers thermocouple data to the mixed-signal test systems with greater feasibility (as shown in Fig. 4(c)).

(v) **Thermal storage unit**
The thermal storage unit is fabricated using different size of stainless-steel plates. In this unit four holes are provided for thermocouples from two opposite sides, and it is confirmed that there is no leakage from any part of the unit. The top face is open and close according to the requirement of replacing the thermal storage material and clean up the unit for a different set of experiments. The complete TSU is well insulated with glass wool material for providing the adiabatic boundary conditions (as shown in Fig. 4(d)).

(vi) **Thermocouples**
The thermocouples used in the experiment are customized with *k*-type temperature sensors of pen type assembly. The dimensions of thermocouples are 3 mm in diameter, 70 mm with 2 m cable length and the temperature range is 0–800 °C. The total number of thermocouples are seven, and namely T_1, T_2, T_3 and T_4 indicates temperatures at different locations of the thermal storage medium, T_5 and T_6 indicates heating base wall and top wall temperature and T_7 indicates the surrounding temperature respectively. All thermocouples are directly connected to the DAQ unit for further recording and computing. The accuracy of K-type thermocouple is ± 0.5 °C or ± 0.75% for temperature range 0 to 200 °C. the uncertainty in power calculation is observed ± 0.5.

(vii) **Computer unit**
Dell Inspiron 15 3543 model laptop (CPU: Intel Core i3-5005 U, GPU: Intel HD Graphics 5500 and RAM: 4GB DDR3) with LabVIEW 2017 is used for recording and computing the data coming from the DAQ unit.

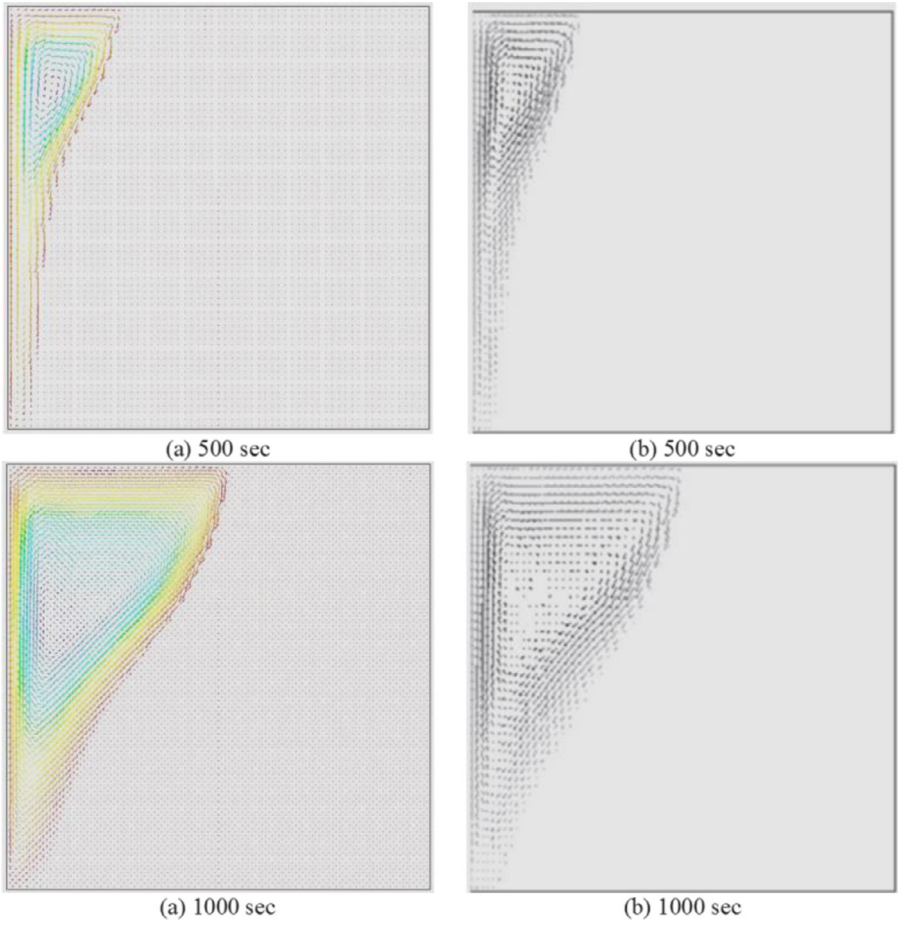

Fig. 2. Streamline patterns (a) Present results and (b) results of Khodadadi et al. [25].

3.3. Materials used and their properties

The thermal storage medium used in this experimental study is prepared and termed as composite phase change materials(CPCMs) such as, CPCM-1, CPCM-2 and CPCM-3 for 1, 3 and 5 wt% of functionalized graphene nanoparticle concentrations. Linear low-density polyethylene (LLDPE) is used as base material for composite preparation to enhance the thermal properties functionalized graphene (f-Gr) nanoparticles are blended. Table 2 shows the list of different materials used in the experiment and their thermo-physical properties.

3.3.1. Heat supply calculations during melting process

Constant rate of heat (250 W) is supplied by controlling the voltage, because voltage is a variable parameter to regulate the heat supply.

$$Q_{supply} = V \times I \tag{5}$$

Total amount of heat supplied is for different time intervals for different materials till it attains the complete molten state. Here V and I are voltage and current in volts and amps respectively as seen in Eq. (1). Throughout the experimental operation temperature variations are recorded under constant heat supply condition.

3.3.2. Analytical heat supply calculations

Amount of heat required for complete melting is calculated using following correlation.

Amount of thermal energy stored = =Amount of heat supplied to raise material temperature from 30 °C (room temperature) to its melting point + Amount of heat supplied during complete phase change + Heat required to increase temperature from melting temperature to maximum temperature.

$$Q = mC_p(T_{melt} - T_{room}) + mH_{fus} + mC_p(T_{max} - T_{melt}) \tag{6}$$

Where Q is the total amount of heat stored, m is mass, $C_p$is Specific heat, H_{fus} is Latent heat of fusion of the CPCM. T_{melt}, T_{room} and T_{max} are melting temperature of CPCM, room temperature and maximum temperature reached during melting process respectively. Experimental, numerical and analytical comparison of heat supplied and time requirement for melting by different materials are listed Table 3.

The amount of heat supplied for complete melting of CPCM is higher for experimental results, compared to numerical and analytical results. The experimental setup contains the different components which absorbs some amount of energy before transferring to the thermal energy storage domain. In numerical study boundary conditions are applied impeccably to the system which transfers heat energy without any leakage. Analytical calculations show low values due to assumptions made for solving the equations. Time requirement during experiment for complete melting is high compared to the numerical analysis due to non-achieving of perfect insulation, and it causes discrepancy between the two results. The amount of heat absorbed during experiment is 1800, 1925, 2050 and 2025 kJ and time taken is 3600, 3850, 4100, 4050 s by LLDPE, CPCM-1, CPCM-2 and CPCM-3 respectively. In numerical analysis, the amount of heat absorbed is 1460, 1570, 1650 and 1610 kJ and time taken for complete melting is 2400, 2600, 3150, 2800 s respectively.

3.3.3. Heat rejection analysis during solidification process

The heat rejection is taking place by combined mode of heat transfer viz convection and radiation.

$$Q_{Total} = Q_{convection} + Q_{radiation} \tag{7}$$

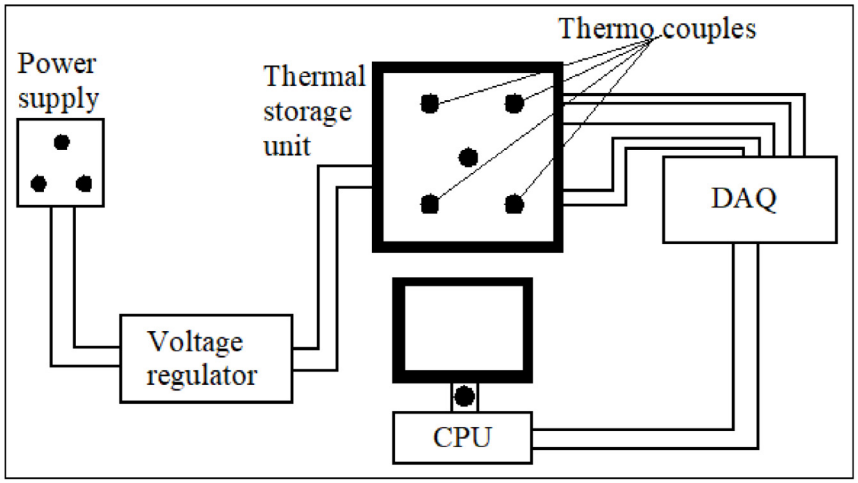

(a) Schematic representation of complete experimental setup.

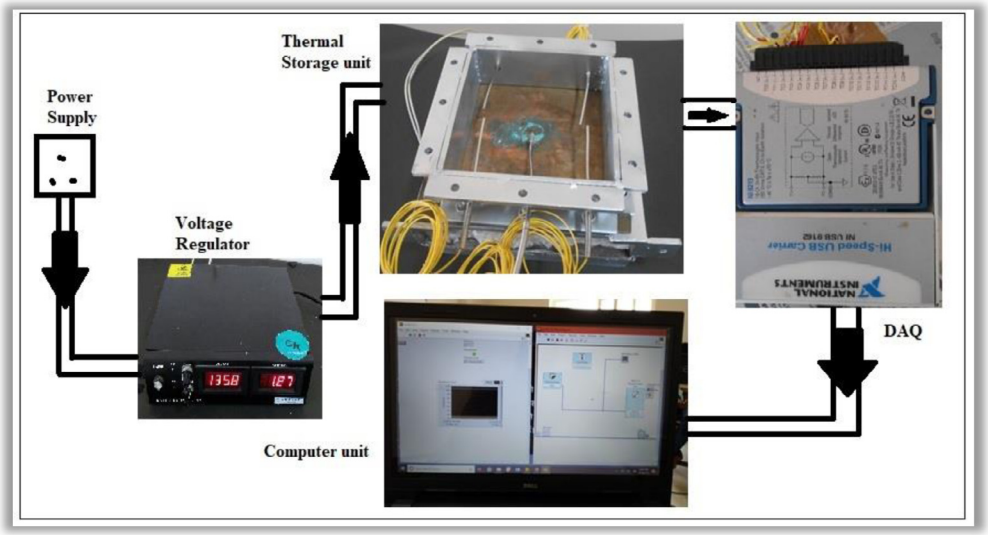

(b) Actual representation of experimental setup.

Fig. 3. Experimental setup of (a) block diagram (b) actual representation.

$$Q_T = (h\,A\,\Delta T) + (\sigma\,A\,\varepsilon)(T_s^4 - T_a^4) \quad (8)$$

Heat transfer through convection

$$Q_c = h\,A\,\Delta T \quad (9)$$

where h is heat transfer coefficient determined by using Nusselt number correlation.

$$h = \frac{Nu \times K}{L} \quad (10)$$

Correlations for heated surface facing upwards given by Mc Adams (1954) and Lloyd & Moron (1974)

$$Nu = 0.54 \times Ra^{1/4} \text{ for } 10^4 < Ra < 10^7$$

$$Nu = 0.15 \times Ra^{1/3} \text{ for } 10^7 < Ra < 10^{10}$$

$$Ra = \frac{g\,\beta\,\Delta T\,L^3}{\nu^2} \times Pr \quad (11)$$

Where g, β,ν, Pr are properties of air at mean temperature T_m. A is area, h is heat transfer coefficient, Nu, Pr and Ra are is Nusselt number, Prandtl number and Rayleigh number.

The mean temperature is given by

$$T_m = \frac{T_s + T_a}{2} \quad (12)$$

Heat transfer through radiation

$$Q_r = \sigma A \varepsilon (T_1^4 - T_2^4) \quad (13)$$

Where σ, A and ε are Boltzmann constant area and emissivity respectively. T_1 and T_2 are surface and wall temperatures, emissivity is also calculated.

The cooling or solidification occurs due to rejection of heat, which is combined effect of convection and radiation. The gradual heat rejection during complete solidification process is estimated for numerical and experimental analysis. Table 4 shows numerical and experimental comparison of heat rejection during solidification. Amount of heat rejection by convection and radiation is calculated for both approaches. Experimental study exhibits high values of rejection compared to numerical results. System efficiency is calculated with respect to the amount of heat supplied during melting, and the amount of heat rejected during the solidification process. The base material shows least rejection and retains 20.53% heat by rejecting 1430.50 kJ of heat, and

(a) Voltage regulator

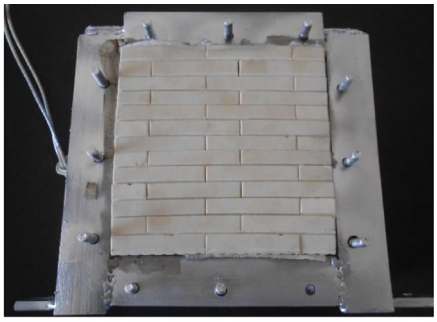

(b) Electric ceramic heater

(c) Data Acquisition system

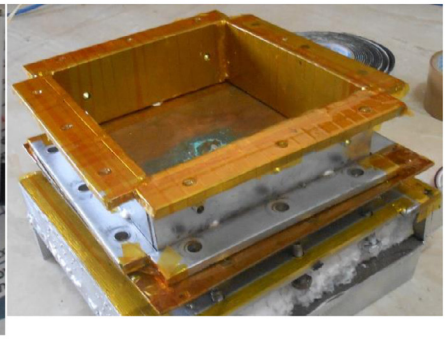

(d) Thermal storage unit

Fig. 4. Experimental Setup components (a) Voltage regulator (b) Electric ceramic heater (c) Data Acquisition system (DAQ) and (d) Thermal storage unit.

CPCM-2 shows maximum rejection and retains 12.90% heat by rejecting 1785.59 kJ of heat. The CPCM-1 and CPCM-3 shows reduction of heat rejection and retains 19.95 and 16.68% by loosing 1541.02 and 1687.25 kJ of heat. The numerical and experimental results are analyzed into two sections (i) heating and (ii) cooling cycle where amount of heat energy stored and temperature variations are summarized.

4. Results and discussion

The numerical and experimental results are analyzed by dividing into two parts (i) heating and (ii) cooling analysis where amount of heat energy stored and temperature variations are analyzed.

4.1. Energy absorption during melting process

Continuous heating is carried out upto 4000 s to complete the melting process. The amount of heat absorbed and rise in temperature is observed and discussed in the present section. Fig. 5 shows numerical and experimental calculation of energy absorbed during melting process with charging for different materials. The heat energy supplied by electric heater at constant rate of 250 W through which the thermal storage material recieves the heat energy, and starts energy level variation during melting process. After 500 s, the heat energy possesed by different materials are 471.13, 754.79, 766.02 and 780.21 kJ calculated for LLDPE, CPCM-1, CPCM-2 and CPCM-3 respectively. As time progresses the continuous supply of heat increases the thermal storage medium temperature till it reaches the phase change temperature. After reaching phase change temperature TSM starts changing its phase and melting begins. This happens without changing surface temperature due to absorption of heat in latent heat form. At the completion of melting process TSM recieves heat upto its saturation limit. Then surface temperature starts to increase as TSM recieves heat in sensible heat form.

To understand the complete melting process, it is divided into 8 time steps with increament of 500 s and values are obtained at those points. At 4000 s, the total energy absorbed and stored by different materials are found to be 1279.45, 1522.61, 1662 and 1580 for LLDPE,

Table 3
Experimental, numerical and analytical comparison of heat supplied and time consumed for melting by different materials.

Materials	Heat supplied for melting (kJ)			Time taken for melting (s)	
	Experimental	Numerical	Analytical	Experimental	Numerical
LLDPE	1800	1460	1144	3600	2400
CPCM-1	1925	1570	1268	3850	2600
CPCM-2	2050	1650	1443	4100	3150
CPCM-3	2025	1610	1302	4050	2800

Table 2
List of different materials used in the experiment and their thermo-physical properties [26].

Materials	Thermo-physical properties Percentage loading (%)	Density (ρ) *(kg/m^3)*	Specific Heat capacity (*Cp*) *(J/kg K)*		Thermal conductivity (*k*) *(W/mK)*		Heat of fusion *(kJ/kg)*	Melting temperature (T_m) (°C)
			Solid	Liquid	Solid	Liquid		
LLDPE	0% f-Gr	928.00	5380	3240	0.320	0.330	71.75	123.00
CPCM-1	1% f-Gr	928.02	3700	2800	0.392	0.351	91.75	122.45
CPCM-2	3% f-Gr	928.05	3680	2600	0.876	0.620	92.90	122.00
CPCM-3	5% f-Gr	929.00	3400	2390	0.886	0.687	97.00	120.00

Table 4
Numerical and experimental comparison of heat rejected during solidification.

Heat rejection during solidification (kJ) Materials	Experimental				Numerical			
	$Q_{Convection}$	$Q_{Radiation}$	Q_{Total}	Heat retention (%)	$Q_{Convection}$	$Q_{Radiation}$	Q_{Total}	Heat retention (%)
LLDPE	972.74	457.76	1430.50	20.53	827.82	306.18	1134	22.32
CPCM-1	983.10	557.92	1541.02	19.95	858.816	405.76	1264.57	19.45
CPCM-2	1273.43	512.16	1785.59	12.90	1160.548	263.72	1424.26	13.68
CPCM-3	1100.95	586.30	1687.25	16.68	942.058	436.4	1378.45	14.38

CPCM-1, CPCM-2 and CPCM-3 respectively. The energy level enhancement of 43.17, 50.42, 54 and 50.61% is recorded for LLDPE, CPCM-1, CPCM-2 and CPCM-3 respectively. Among the TSM CPCM-2 shows relatively better storage capability (54% enhancement) due to incorporation of optimum concentration of enhancing material. Higher concentration causes reduction in specific heat capacity of CPCM-3 and it leads to reduction in thermal storability. The discrepancy between numerical and experimental results are due to insulation of thermal storage unit, measurement device and operating conditions.

4.2. Temperature variation during melting process

The temperature variation during phase change process is monitored and found in the initial stage of phase change process. The average temperature in simulation is slightly uniform for all TSMs. Experimental temperature values are higher for LLDPE and CPCM-1, but CPCM-2 and CPCM-3 temperature is lower than numerical results with increase in heating plate temperature. As time progresses the viscous properties of the material, temperature of CPCM-2 and CPCM-3 increases rapidly due to its higher thermal conductivity. Blending of high conductive material changes thermophysical properties and thermal performance enhances.

Fig. 6 shows the numerical and experimental calculation of temperature variation during melting process with charging time for different materials. The temperature variation data shows the temperature increment of 28, 24, 50 and 52.73% for LLDPE, CPCM-1,CPCM-2 and CPCM-3 respectively.

4.3. Energy rejection and temperature variation during the solidification process

The complete solidification process requires 40,000 s, and it is divided into 8-time steps with increment of 5000 s to understand the solidification process. The heat rejection process is by natural convection and required longer time to complete the process. The numerical and experimental calculations of energy rejection during solidification process with discharging time for different materials are as shown in Fig. 7. A comparative study of numerical and experimental results are different, but it follows the same trend. At the beginning of solidification process, the amount of heat energy stored in the TSM is 1279.45, 1522.61, 1662.09 and 1580.02 kJ calculated for LLDPE, CPCM-1,CPCM-2 and CPCM-3 respectively.

The TSM is kept open to atmosphere heat rejection takes place through natural convection and considerable amount of heat is rejected through radiation. The total heat rejection leads to energy level drop in the TSM and as time progresess heat rejection process is continuous until reaches the surrounding temperature. At the completion of solidification process the TSM energy level reduces 79.47, 80.05, 87.10 and 83.32% for LLDPE, CPCM-1,CPCM-2 and CPCM-3 respectively.

Fig. 8 shows numerical and experimental calculations of temperature variation during solidification process with discharging time for different materials. The temperature variation is high in experiment but it is uniform for numerical analysis, and the percentage variation is ranging between 11 and 23%. The temperature percentage reduction is 44, 46, 53.6 and 49.53% for LLDPE, CPCM-1,CPCM-2 and CPCM-3 respectively.

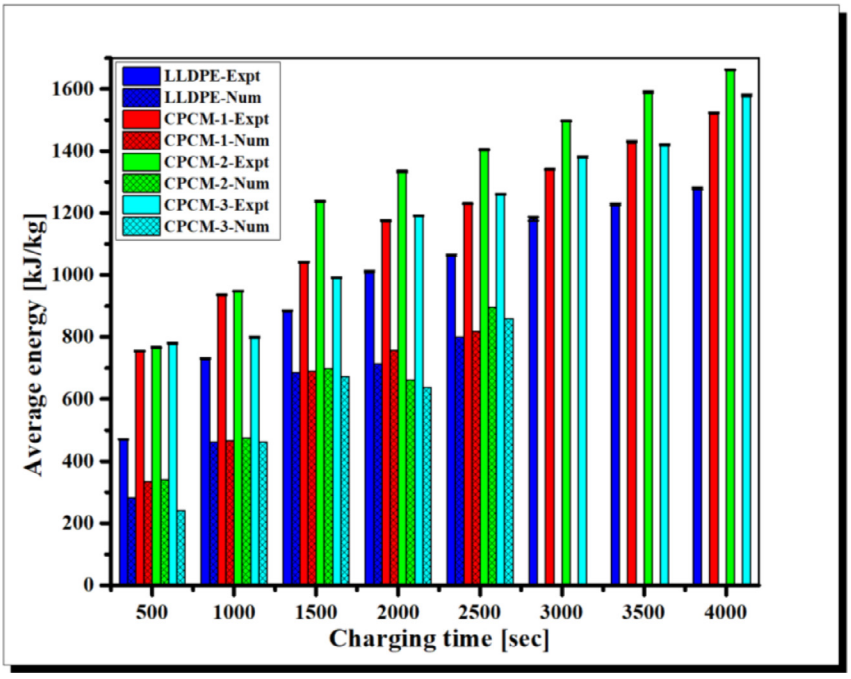

Fig. 5. Numerical and experimental estimation of energy absorbed during melting process with charging time for different materials.

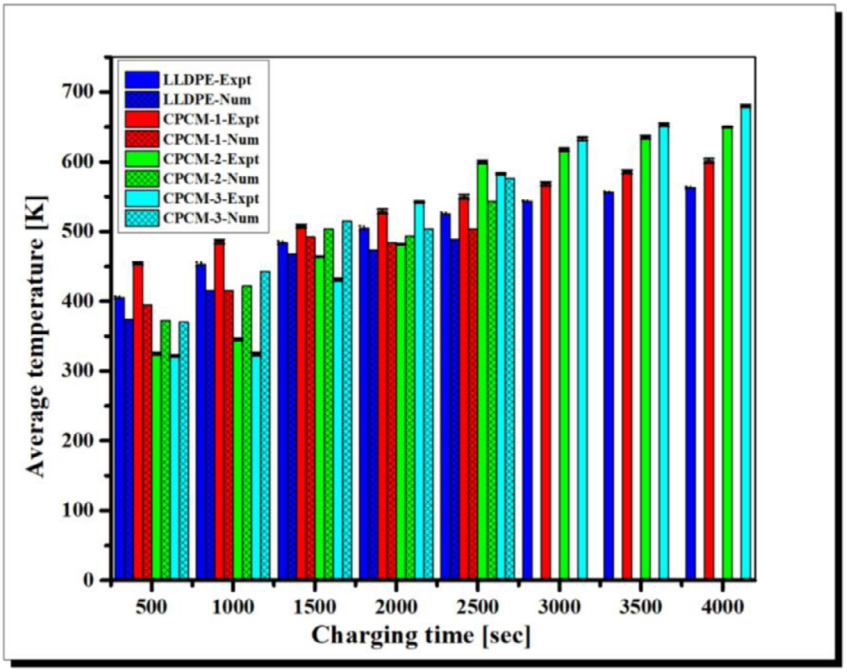

Fig. 6. Numerical and experimental estimation of temperature variation during melting process with charging time for different materials.

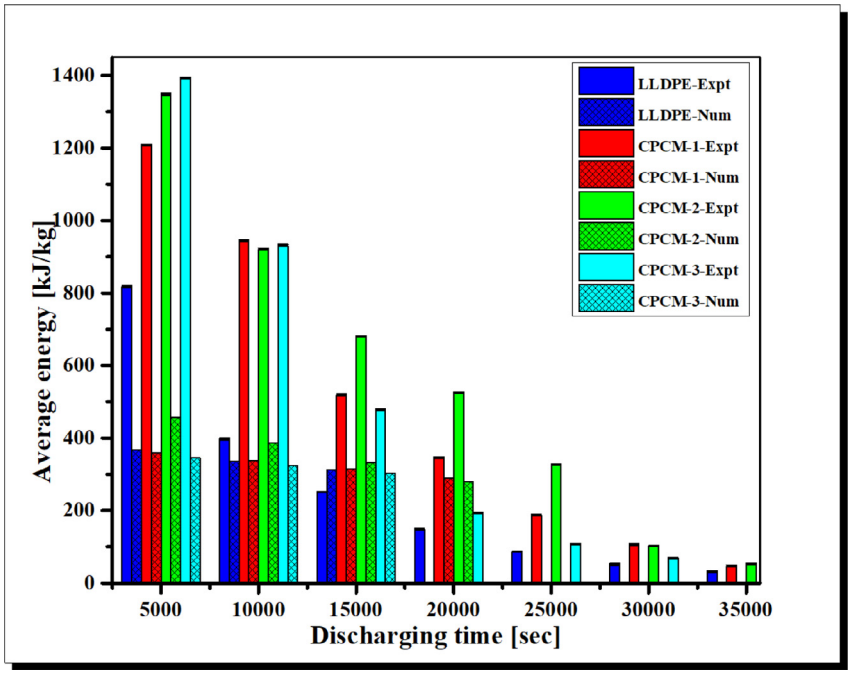

Fig. 7. Numerical and experimental calculation of energy rejection during solidification process with discharging time for different materials.

The maximum temperature loss is 53.6% for CPCM-2. Good agreement is seen for temperature variation between numerical and experimental results. The discrepancy is observed at the beginning of the solidification process, and it is due to conduction resistance ignored for numerical studies. This resistance causes reduction in heat transfer rate and holds heat energy within the TSM and surface temperature is maintained constant throughout the process.

4.4. Total heat rejection analysis

Thermophysical properties of TSM play a significant role in storing heat energy, such as thermal conductivity and viscosity respectively. Materials with high thermal conductivity leads faster charging and discharging rate, same materials with high viscosity resists the particle migration during convection and controls the heat transfer rate.

Fig. 9 shows numerical and experimental estimation of convection, radiation and total heat transfer contribution during solidification process for different materials. In the total amount of heat transfer, natural convection heat transfer contributes more and the radiation effect subsidizes considerable amount of heat. The convection heat transfer is calculated as 71.43, 69.45, 80 and 68.96% for LLDPE, CPCM-1,CPCM-2 and CPCM-3 respectively. Radiation heat loss contributes 28.57, 30.55, 20 and 31.03% for LLDPE, CPCM-1,CPCM-2 and CPCM-3 respectively. Maximum heat rejection is observed for CPCM-2 around

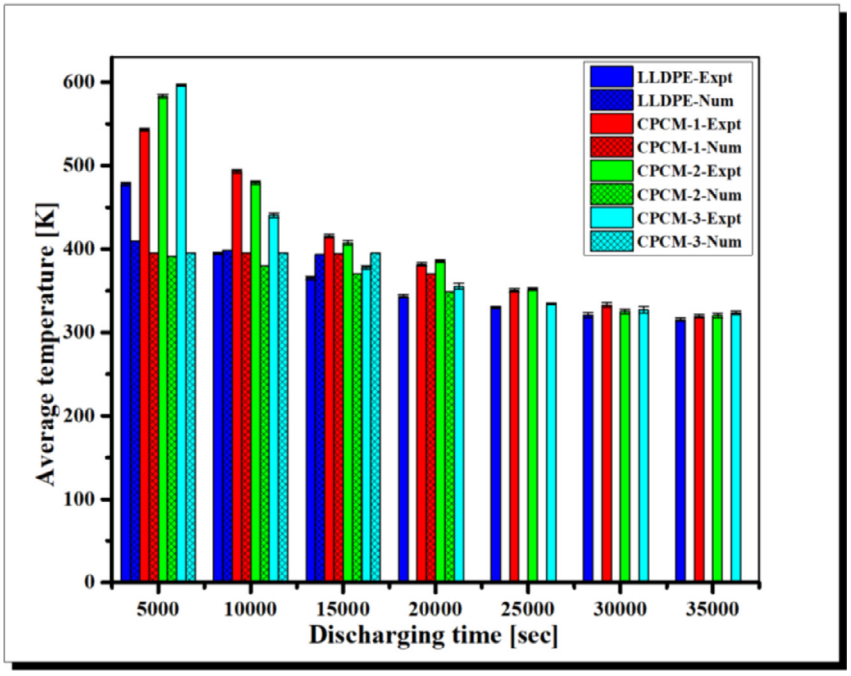

Fig. 8. Numerical and experimental calculation of temperature variation during solidification process with discharging time for different materials.

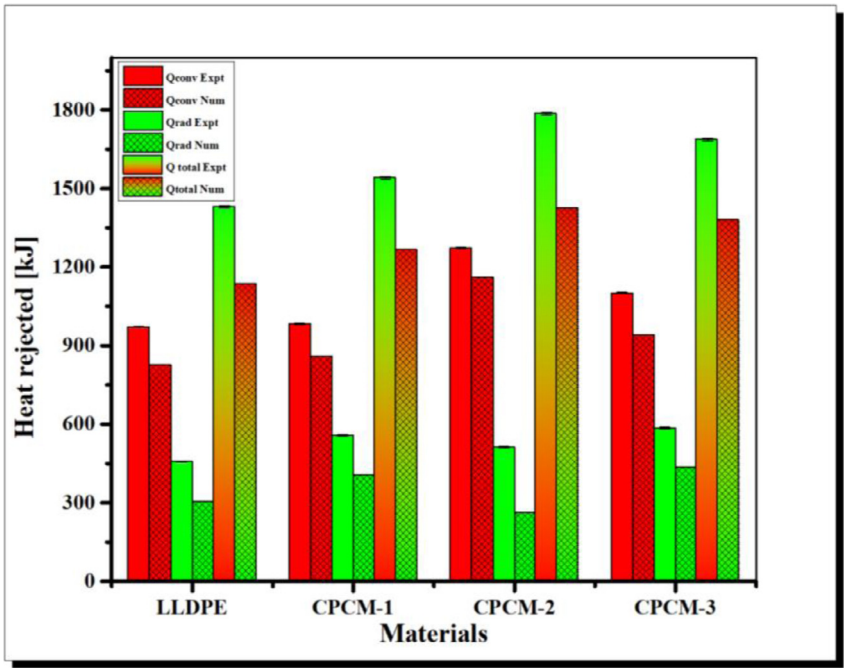

Fig. 9. Numerical and experimental calculation of convection, radiation and total heat transfer contribution during solidification process for different materials.

75% numerically and 80% experimentally.

4.5. Heating and cooling cycle analysis

The amount of heat energy stored during melting process is calculated by the amount of heat energy transferred from heating plate to thermal storage material. Total energy supplied is the time integration of the instantaneous heat transfer rate during the melting process. Fig. 10 shows the numerical and experimental comparison of energy stored and rejected during complete cycle with time for different thermal storage materials. Initially, sharp increment of curve is observed which indicates sensible heating of TSM up to phase change temperature. It follows a plateau of gradual increase in energy level and it reaches to the saturation point above which phase change occurs. The CPCM-2 reaches highest peak by absorbing 1662 kJ of heat. The consequent peaks are obtained at 1279.45, 1522.61, 1662 and 1580 kJ for LLDPE, CPCM-1,CPCM-2 and CPCM-3 respectively and completes the melting process at 4000 s.

As TSM reaches the molten phase heat supply is stopped and top surface is kept open to allow heat rejection through natural convection. More heat rejection takes place by natural convection but total heat rejection takes place by convection and radiation mode of heat transfer. Radiative heat loss subsidizes around 20 to 30%. The declining trend of curves shows the solidification process, and these curves are shorter for

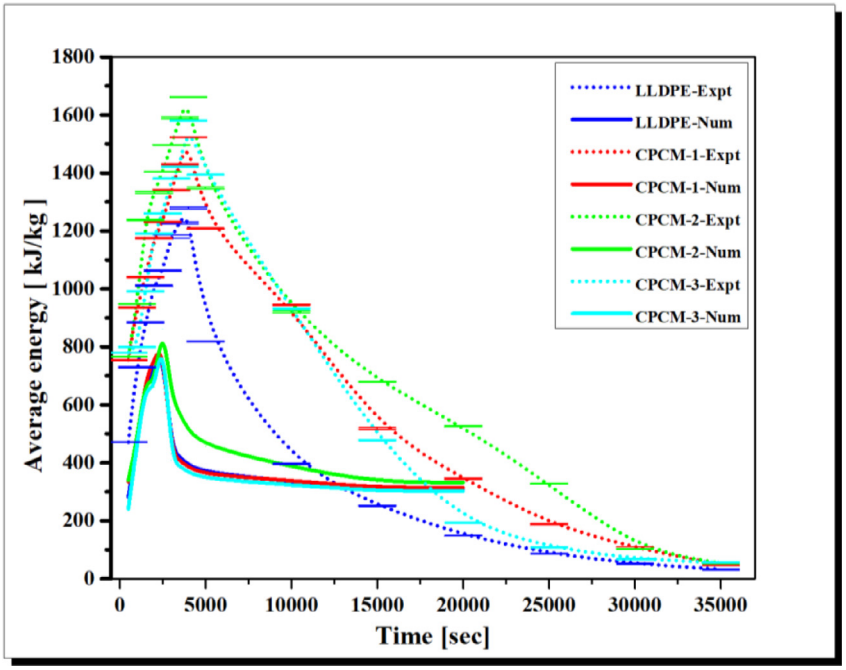

Fig. 10. Numerical and experimental comparison of energy stored and released during complete cycle with time for different thermal storage materials.

numerical compared to experimental results. The complete system is considered to be perfectly insulated and amount of heat released from heater is completely absorbed by the materials without any thermal loss. During experiment perfect insulation is not possible and some amount of heat absorbed by thermal storage unit itself due to its material properties. Several unavoidable conditions also makes the discrepancy between numerical and experimental results. The curves obtained through simulation are shorter than experimental curves because the amount of heat energy supplied to the TSM is completely transferred.

Fig. 11 shows numerical and experimental comparison of temperature variation during complete cycle with time for different thermal storage materials. During solidification process TSM rejects heat faster and requires less time compared to experimental results. In numerical analysis solidification process completes within 20,000 s of time interval but experiment completes 40,000 s of time. As TSM loses the sensible heat, material temperature starts declining untill it reaches the phase change temperature.

The instantaneous energy level is ascended to maximum energy level under the given operating conditions, in order to compare the results for both numerical and experimental results. It is clear that, higher temperature differences leads to faster charging and discharging of sensible heat and it affects the themal energy storage performance.

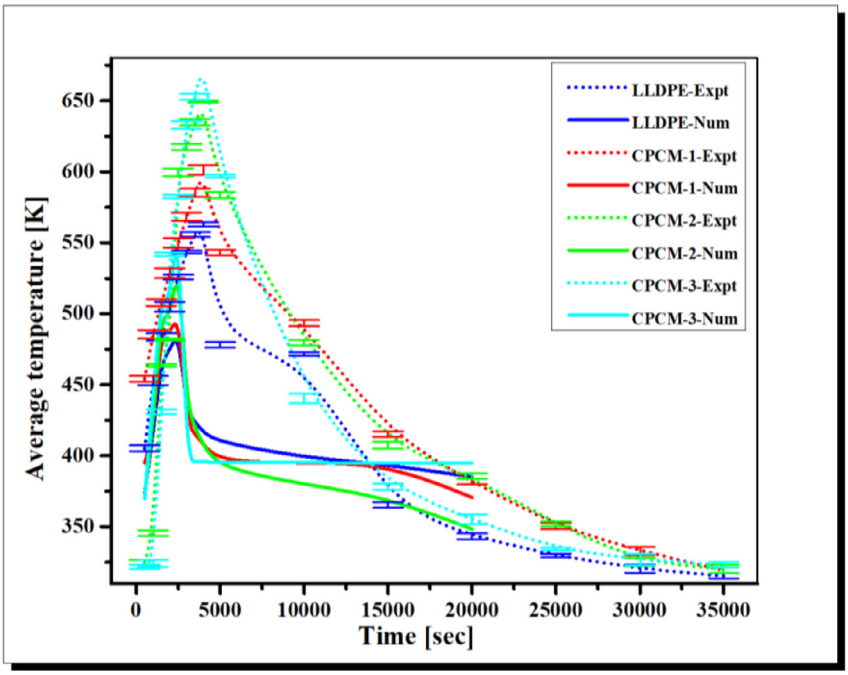

Fig. 11. Numerical and experimental results comparison of temperature variation during complete cycle with time for different thermal storage materials.

4.6. Unceratinty analysis

The uncertainty is assessed using the three sample readings measured during the experimentation. Through these measurements average values are calculated and finally standard deviation is also determined. Uncertainty is calculated using following formula.

$$\sigma = \sqrt{\frac{\sum_{i=1}^{N} (X_i - \bar{X})^2}{N-1}} \quad (14)$$

$$\bar{X} = \frac{X_1 + X_2 + X_3 \ldots}{N} \quad (15)$$

Where X_i is Sample, $\bar{X} = =$ Average sample values, and N is the number of samples.

The uncertainty is obtained for temperature measurement is 0.202 and for energy it is 0.543. The uncertainty in measuring the convective heat transfer is 2.5 and the radiative heat transfer is 4.38. The uncertainty in measuring temperature is estimated the values 0.202041, 0.459342, 0.835275 and 0.553831 for LLDPE, CPCM-1, CPCM-2 and CPCM-3 respectively. There is uncertainty observed in calculating the thermal energy storage capacity of different materials and the uncertainties are 0.543252, 0.426386, 0.616323 and 0.70450 for LLDPE, CPCM-1, CPCM-2 and CPCM-3 respectively.

5. Conclusion

The present work successfully demonstrates the feasibility and applicability of plastic based composite phase change materials (CPCMs) using polyethylene as base material for thermal energy storage applications. Numerical and experimental investigation are carried out to evaluate thermal performance of four thermal storage materials/composite phase change materials such as, LLDPE, CPCM-1,CPCM-2 and CPM-3. Thermal characteristic response such as, thermal energy storage capacity, charging and discharging time, temperature variation during melting and solidification process are examined. Through the observations following conclusions are drawn.

- The energy level enrichment is 43.17, 50.42, 54 and 50.61% for LLDPE, CPCM-1, CPCM-2 and CPCM-3 respectively.
- The temperature increases from 28, 24, 50 and 52.73% for LLDPE, CPCM-1,CPCM-2 and CPCM-3 respectively. During solidification process the temperature reduces 44, 46, 53.6 and 49.53% for LLDPE, CPCM-1,CPCM-2 and CPCM-3 respectively.
- Enhanced thermal storage capacity is achieved through optimum percentage blending (3%) and waste polyethylene can be successfully converted into thermal storage material.
- The functionalized graphene significantly improved the thermophysical properties of polyethylene, it is demonstrated that waste plastics can be manipulated and it can be used for TES application like solar thermal storage.

This present work also addresses the global issues of energy preservation and controlling the plastic pollution in the environment with cost reduction. TES model implementation also determines the better utilization of thermal energy for a greener environment. It will be very obliging in tackling with energy issues and environmental pollution caused due to usage of plastics.

Declaration of Competing Interest

None.

References

[1] X. Xu, X. Zhang, J.M. Munyalo, Key technologies and research progress on enhanced characteristics of cold thermal energy storage, J. Mol. Liq. 278 (2019) 428–437.
[2] A. Dahash, F. Ochs, M.B. Janetti, W. Streicher, Advances in seasonal thermal energy storage for solar district heating applications : a critical review on large-scale hot-water tank and pit thermal energy storage systems, Appl. Energy 239 (October 2018) (2019) 296–315.
[3] V. Koushal, R. Sharma, M. Sharma, R. Sharma, V. Sharma, Plastics : issues challenges and remediation, Int. J. Waste Resour. 4 (1) (2014) 1–6.
[4] X. Lu, J. Huang, B. Kang, T. Yuan, J. Qu, Bio-based poly (lactic acid)/ high-density polyethylene blends as shape- stabilized phase change material for thermal energy storage applications, Sol. Energy Mater. Sol. Cells 192 (2019) 170–178.
[5] J.C. Thermodynamics, et al., Thermal analysis and heat capacity study of polyethylene glycol (PEG) phase change materials for thermal energy storage applications, J. Chem. Thermodyn. 128 (2019) 259–274.
[6] N. H., B. M., F. J., M. Bolivar, X. Isaza-ruiz, K. Xu, P. Vignarooban, Phelan, A.M. Kannan, Recent developments in phase change materials for energy storage applications : a review, Int. J. Heat Mass Transf. 129 (2019) 491–523.
[7] K.Y. Leong, M. Rosdzimin, A. Rahman, B.A. Gurunathan, Nano-enhanced phase change materials : a review of thermo-physical properties, applications and challenges, J. Energy Storage 21 (2019) 18–31.
[8] J.A. Molefi, A.S. Luyt, I. Krupa, Comparison of LDPE, LLDPE and HDPE as matrices for phase change materials based on a soft Fischer – Tropsch paraffin wax, Thermochim. Acta 500 (1–2) (2010) 88–92.
[9] Y. Zhang, L. Wang, B. Tang, R. Lu, S. Zhang, Form-stable phase change materials with high phase change enthalpy from the composite of paraffin and cross-linking phase change structure, Appl. Energy 184 (2016) 241–246.
[10] S. Chavan, V. Gumtapure, D.A. Perumal, A review on thermal energy storage using composite phase change materials, Recent Pat. Mech. Eng. 11 (2018) 1–13.
[11] H.M. da Costa, V.D. Ramos, Analysis of thermal properties and rheological behavior of LLDPE/EPDM and LLDPE/EPDM/SRT mixtures, Polym. Test. 27 (1) (2008) 27–34.
[12] H.A. Khonakdar, Dynamic mechanical analysis and thermal properties of LLDPE/EVA/modified silica nanocomposites, Compos. Part B Eng. 76 (2015) 343–353.
[13] P. Sobolciak, M. Karkri, I. Krupa, M. Al Maadeed, Storage and release of thermal energy of phase change materials based on linear low density of polyethylene, parafin wax and expanded graphite, 0 Proc. TMS Middle East - Mediterr. Mater. Congr. Energy Infrastruct. Syst. MEMA 2015, 2015.
[14] Vinh Duy Cao, Shima Pilehvara, Carlos Salas-Bringas, Anna M. Szczotok, Tri Quang Bui, Manuel Carmona, Juan F. Rodriguez, Anna-Lena Kjøniksen, Thermal analysis of geopolymer concrete walls containing microencapsulated phase change materials for building applications, Sol. Energy 178 (2019) 295–307.
[15] Y. Zhang, G.G. Gurzadyan, M.M. Umair, W. Wang, R. Lu, Ultrafast and efficient photothermal conversion for sunlight-driven thermal- electric system, Chem. Eng. J. 344 (2018) 402–409.
[16] M. Mumtaz, A. Khan, N.I. Ibrahim, I.M. Mahbubul, R. Saidur, F.A. Al-sulaiman, Evaluation of solar collector designs with integrated latent heat thermal energy storage : a review, Solar Energy 166 (2018) 334–350.
[17] H. Muhammad, A. Arshad, Experimental investigation of n-eicosane based circular pin-fin heat sinks for passive cooling of electronic devices, Int. J. Heat Mass Transf. 112 (2017) 649–661.
[18] H. Muhammad, A. Arshad, M. Jabbal, P.G. Verdin, Thermal management of electronics devices with PCMs filled pin-fin heat sinks : a comparison, Int. J. Heat Mass Transf. 117 (2018) 1199–1204.
[19] A. Arshad, H. Muhammad, S. Khushnood, M. Jabbal, Experimental investigation of PCM based round pin-fin heat sinks for thermal management of electronics : effect of pin-fin diameter, Int. J. Heat Mass Transf. 117 (2018) 861–872.
[20] H. Muhammad, A. Arshad, M. Mansoor, W. Baig, U. Sajjad, Thermal performance of LHSU for electronics under steady and transient operations modes, Int. J. Heat Mass Transf. 127 (2018) 1223–1232.
[21] T.- Rehman, H. Muhammad, A. Saieed, W. Pao, M. Ali, Copper foam / PCMs based heat sinks : an experimental study for electronic cooling systems, Int. J. Heat Mass Transf. 127 (2018) 381–393.
[22] Z.A. Qureshi, H.M. Ali, S. Khushnood, Recent advances on thermal conductivity enhancement of phase change materials for energy storage system : a review, Int. J. Heat Mass Transf. 127 (2018) 838–856.
[23] I.M. Mahbubul, M. Mumtaz, A. Khan, N.I. Ibrahim, F.A. Al-sulaiman, R. Saidur, Carbon nanotube nano fluid in enhancing the efficiency of evacuated tube solar collector, Renewable Energy 121 (2018) 36–44.
[24] S. Chavan, V. Gumtapure, D.A. Perumal, Computational investigation of bounded domain with di ff erent orientations using CPCM, J. Energy Storage 22 (2019) 355–372.
[25] J.M. Khodadadi, S.F. Hosseinizadeh, Nanoparticle-enhanced phase change materials (NEPCM) with great potential for improved thermal energy storage, Int. Commun. Heat Mass Transf. 34 (2007) 534–543.
[26] S. Chavan, V. Gumtapure, D.A. Perumal, Characterization of linear low-density polyethylene with graphene as thermal energy storage material characterization of linear low-density polyethylene with graphene as thermal energy storage material, Mater. Res. Express 6 (2019) 1–9.